NAG-1-330

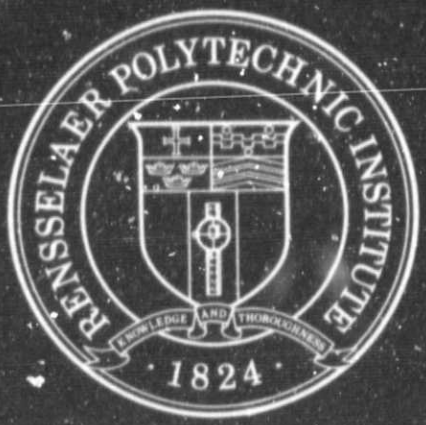

Rensselaer Polytechnic Institute

Troy, New York 12181

FOREWORD

This report was prepared under NASA Grant No. NAG-1-330 for the NASA Langley Research Center under the technical direction of Dr. L. Maestrello. The work was conducted at the Transonic and Supersonic Wind Tunnel Laboratory, Rensselaer Polytechnic Institute in Troy, New York.

INVESTIGATION TO OPTIMIZE THE PASSIVE SHOCK WAVE/BOUNDARY LAYER CONTROL FOR SUPERCRITICAL AIRFOIL DRAG REDUCTION

by

H.T. Nagamatsu and R. Dyer

Final Report
NASA Grant No. NAG-1-330
NASA Langley Research Center

Department of Mechanical Engineering,
Aeronautical Engineering & Mechanics
Rensselaer Polytechnic Institute
Troy, NY 12181

December 1984

TABLE OF CONTENTS

ABSTRACT

An investigation of the passive shock wave/boundary layer control for reducing the drag of 14%-thick supercritical airfoil was conducted in the 3 in. x 15.4 in. RPI Transonic Wind Tunnel with and without the top wall insert at transonic Mach numbers. Top wall insert was installed to increase the flow Mach number to 0.90 with the model mounted on the test section bottom wall. Various porous surfaces with a cavity underneath was positioned on the area of the airfoil where the shock wave occurs. The higher pressure behind the shock wave circulates flow through the cavity to the lower pressure ahead of the shock wave. The effects from this circulation prevent boundary layer separation and enthropy increase through the shock wave.

The static pressure distributions over the airfoil, the wake impact pressure survey for determining the profile drag and the Schlieren photographs for porous surfaces are presented and compared with the results for solid surface airfoil. With a 2.8% uniform porosity the normal shock wave for the solid surface was changed to a lambda shock wave, and the wake impact pressure data indicated a drag coefficient reduction as much as 45% lower than for the solid surface airfoil at high transonic Mach numbers.

NOMENCLATURE

a	acoustic velocity
C	airfoil chord
C_d'	point drag coefficient
C_d	section drag coefficient
C_p	specific heat at constant pressure
h	vertical distance
H	local total pressure in wake
M	Mach number
P	pressure
R	gas constant
S	entropy
u	flow velocity
x	axial distance
β	shock wave angle
θ	flow deflection
ρ	density
γ	ratio of specific heats

Subscripts

1	condition upstream of shock wave
2	condition downstream of shock wave
o	stagnation property
∞	free stream condition

1. INTRODUCTION

The worldwide demand for more fuel efficient air transport calls for innovative ideas in refining designs and improving aerodynamic characteristics. One such idea is to reduce transonic wave drag due to the supersonic flow over airfoils by a method known as Passive Shock Wave/Boundary Layer Control. In the transonic flight regime a large increase in the wing drag occurs as the drag divergence Mach number is exceeded. The supercritical airfoils [1,2] are shaped to delay the drag rise associated with the energy losses caused by shock waves and flow separation, but for these airfoils the drag also increases rapidly for speeds greater than the design Mach number.

To control the drag increase due to the shock wave/boundary layer interaction for conventional and supercritical airfoils, a basic research program on the passive drag reduction was initiated at the Rensselaer Polytechnic Institute at the suggestion of Mr. Dennis Bushnell and Dr. Richard Whitcomb at the NASA Langley Research Center in the Transonic Wind Tunnel, Figs. 1 and 2. The concept of the passive drag reduction consists of having a porous surface with a cavity underneath at the shock wave location. By this method the boundary layer will thicken ahead of the normal shock wave and produce an oblique shock wave at the leading edge of the porosity. The Mach number ahead of the normal shock wave will approach sonic and the boundary layer downstream of the shock is made thinner which decreases the boundary layer separation region, Fig. 3. Both of these effects tend to decrease the drag at transonic speeds.

The concept was shown to be effective at transonic Mach numbers for a circular airofil by Ross [3] and for a 14%-thick NASA supercritical airfoil by Bahi and Nagamatsu [4,5] and Bidlack [6]. The objectives of the study

were to obtain more detailed information regarding the shock wave/boundary layer interaction phenomena with the porous surfaces and to investigate the effects of linear and uniform porosity distributions on the drag reduction of supercritical airfoil. The results from the investigation are presented in the paper.

Orozco's work [7,8] in particular, revealed that a 46% drag reduction on the supercritical airfoil is possible but choking problems in the test section of the RPI Transonic Wind Tunnel prevented data collection at Mach numbers greater than .82. This prompted the installation of a top wall insert in the tunnel test section to minimize choking and raise the maximum tunnel Mach number to .90. The objective of this paper was to investigate passive shock wave/boundary layer control on the 14%-thick supercritical airfoil in the enlarged freestream Mach number range of .75 to .90 [9,10].

2. EXPERIMENTAL FACILITY AND INSTRUMENTATION

2.1 Transonic Wind Tunnel

The RPI Transonic Wind Tunnel used in this investigation is a conventional blow-down wind tunnel with an atmospheric air intake. The original 3 in. x 15.4 in. test section was modified with the addition of a mahogany top wall insert for the reasons described earlier. Figure 1a is a photograph of the tunnel. The test section side walls are made of 1.25 in. thick clear Plexiglas with aluminum plates attached for stiffness. Half-circles of 4.25 in. diameter were cut from the aluminum plates to permit Schlieren photographs of the shock waves present on the airfoil at transonic speeds (cf. Fig. 1b). The tunnel boundary layer on the bottom of the test section is removed through a narrow opening in front of the airfoil that is connected to the vacuum system (cf. Fig. 2a). The airfoil model is mounted on the

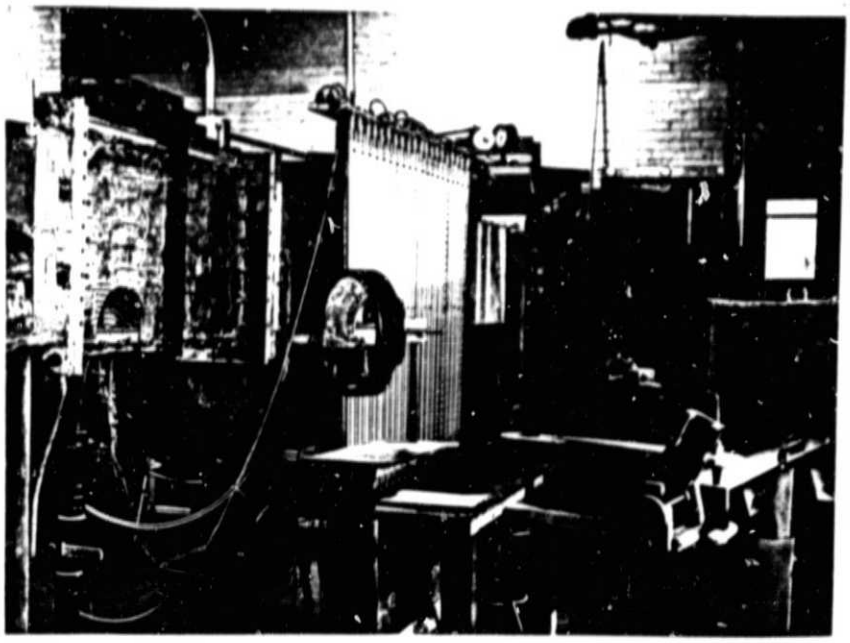

Fig. 1a Photograph of Transonic Wind Tunnel

bottom wall of the test section approximately 6 in. from the inlet. An adjustable wedge is positioned near the test section exit to change the tunnel flow Mach number by changing the ratio of the test to throat area A/A*.

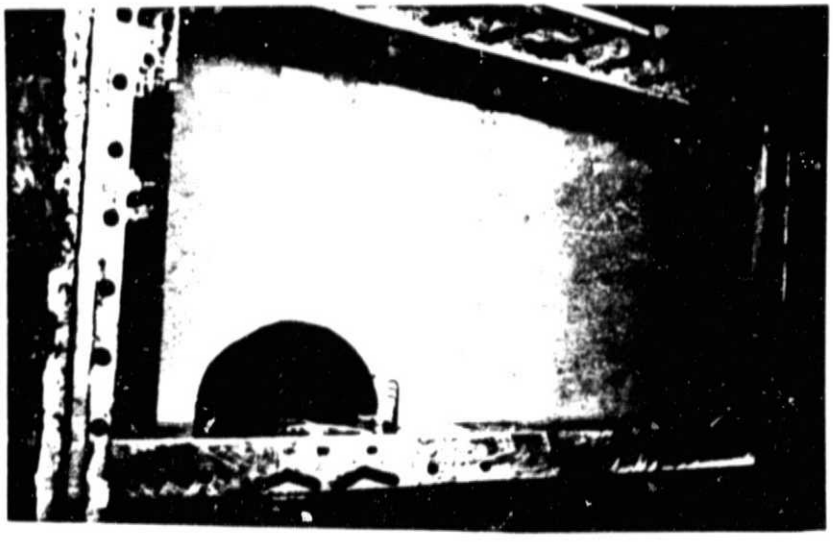

Fig. 1b Photograph of Test Section

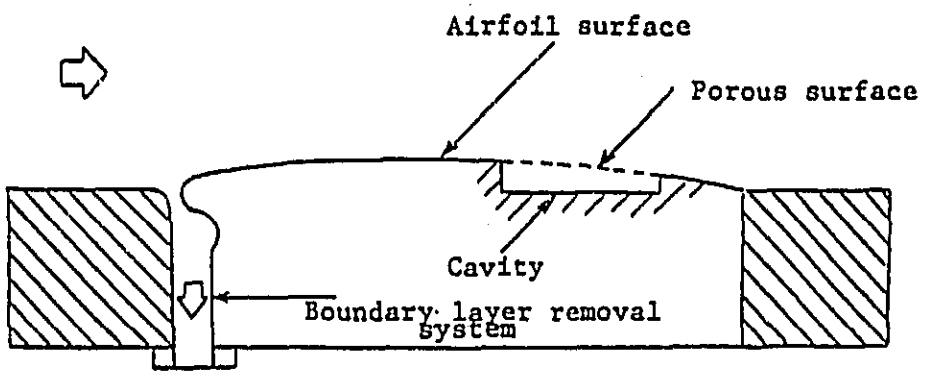

Fig. 2a Schematic of Airfoil Model in Test Section

2.2 Top Wall Insert

The design and construction of a mahogany top wall insert was prompted by the inability of the tunnel to reach Mach numbers above .83. The cause of this problem is the sensitivity of the local Mach number to slight variations in the local area ratio A/A* in the transonic region. It was found that blockage effects from the model combined with the boundary layer build-up on the walls caused the flow to choke at unpredictable locations. These effets were taken into account in the contouring of the insert and the tunnel Mach number was raised beyond .90 (cf. Fig. 4).

2.3 Instrumentation

Static pressure taps are located throughout the test section and a total pressure probe is located in the settling chamber. In addition the airfoil model's wake impact pessures are measured using a stainless steel total pressure rake located 1.75 in. behind the trailing edge of the model. All of these taps can be connected to 22 mercury filled U-tube manometers located alongside the tunnel, as shown in Fig. 1a.

A key activated electrical timing system controls the opening and closing of the large pneumatic valve that allows flow through the tunnel, the triggering of a camera and the locking of solenoid valves on the mercury manometers.

A single pass Schlieren optical system was used to observe the shock waves over the airfoil. This system employs a zirconium light source, two 7.5 in. diameter parabolic mirrors, two 9.5 in. diameter flat mirrors and an adjustable knife edge. A camera box behind the knife edge allows for photographs. It should be noted that the dark regions appearing at the leading and trailing edges of the model are caused by stress concentrations in the Plexiglas side walls. Also, the dark circular region appearing well above the model is caused by scratches in the Plexiglas.

2.4 14% Thick Supercritical Airfoil

An aluminum 14% thick NASA supercritical airfoil [7] was used in this investigation. This model was cut on a computerized milling machine that employed a 200 point upper surface profile. The chord is 4 in. and the span is 3 in. Sixteen static pressure taps are positioned along the centerline of the model top surface (cf. Figs. 2b, c).

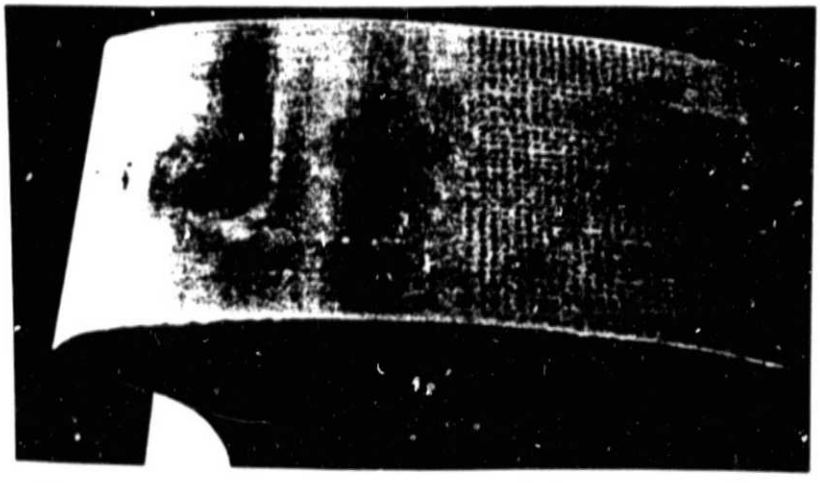

Fig. 2b Photograph of Supercritical Airfoil Model

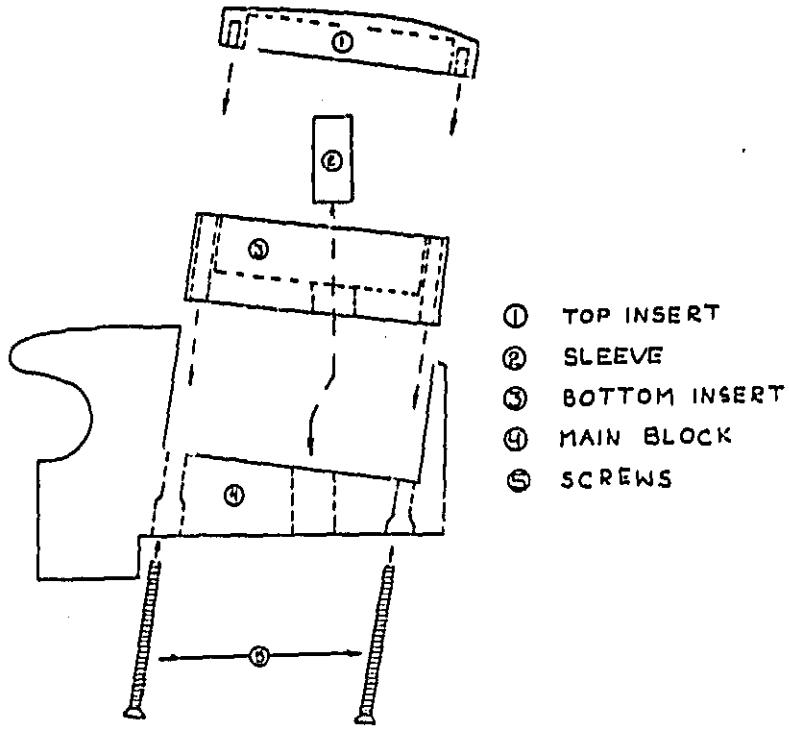

Fig. 2c Assembly Diagram of Supercritical with Removeable Insert

The porous region on this model extends from 56% to 83% of the chord. The holes have a diameter of 0.025 in. and are spaced in 18 rows of 38 holes each. The porosity based on the hole area divided by the total airfoil area is 2.8% with all of the holes open. The case when all of the holes are plugged is referred to as a 0% porosity or solid surface airfoil. The porosity based on the hole area divided by the area between the 56% and 83% marks is 10.4%. Distribution of the holes in the chordwise direction can be varied from uniform to linearily-increasing by selectively opening and blocking the holes with paraffin wax [7,8].

The cavity located under the porous surface is 3/4 in. deep and can be partially filled to obtain different cavity depths. A 1/4 in. cavity, which was found by Bahi [4] to be more effective than the deeper cavity of 3/4 in., was selected and kept constant throughout this investigation.

1. Supercritical airfoil
2. Porous surface
3. Cavity beneath porous surface
4. Free stream conditions
5. Embedded supersonic region
6. Sonic line
7. Terminating shock wave
8. Flow circulation through the porous surface
9. Wake survey rake

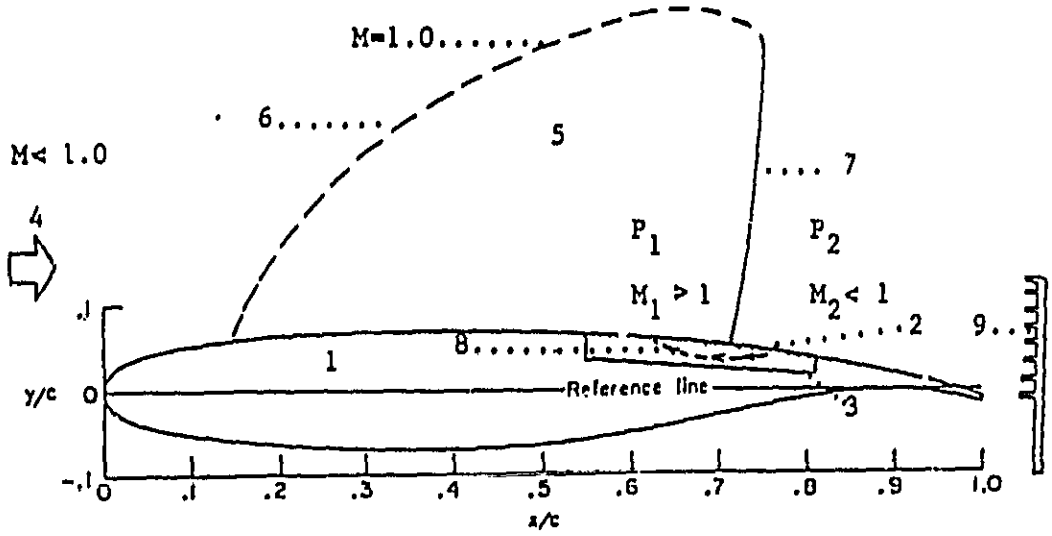

Fig. 3 Diagram of Passive Drag Control Concept

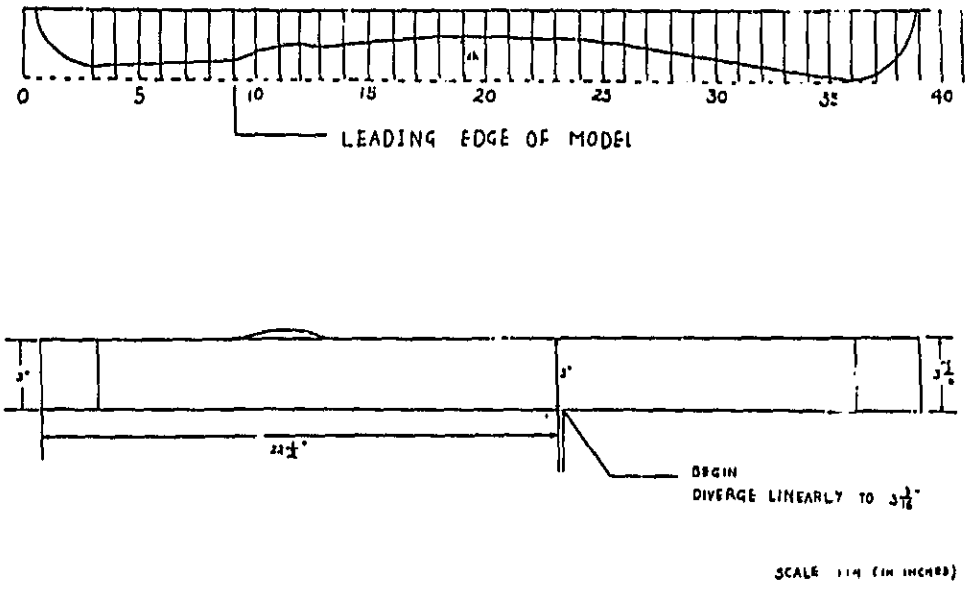

Fig. 4 Transonic Tunnel Top Wall Insert

3. THEORY

The basic compressible flow equations used in the present research program for the data reduction are presented in this section for the assumption of steady, perfect gas flow [11,12].

3.1 Isentropic Flow Equations

3.1.1 Determination of Mach Number

The Mach number in the test section, over the model surface and throughout the tunnel, was obtained from measurements of the static pressure, P, and the total pressure in the settling chamber, P_o. The Mach number is then given by the well-known compressible isentropic flow relations [11].

$$\frac{P}{P_o} = \left[1 + \left(\frac{\gamma-1}{2} M^2\right)\right]^{-\frac{\gamma}{\gamma-1}} \tag{1}$$

where $\gamma = C_p/C_v$ was taken as 1.400.

3.1.2 Determination of the Pressure Coefficients

For an isentropic flow, the pressure coefficient is given by

$$C_p = \frac{2}{\gamma M_\infty^2}\left(\left[\frac{2 + (\gamma-1)M_\infty^2}{2 + (\gamma-1)M^2}\right]^{\frac{\gamma}{\gamma-1}} - 1\right) \tag{2}$$

where M_∞ is the free stream Mach number ahead of the model and M is the local Mach number obtained from Eq. (1).

3.2 Normal and Oblique Shock Wave Relations

3.2.1 Normal Shock Wave Relations

The relation between the Mach number upstream and downstream of the normal shock wave is given by

$$M_2^2 = \frac{(\gamma-1)M_1^2 + 2}{2\gamma M_1^2 - (\gamma-1)} \tag{3}$$

where the subscripts 1 and 2 define the conditions upstream and downstream of the shock wave. The ratio of the static pressure is often used to define the shock wave strength and is given by

$$\frac{P_2}{P_1} = 1 + \frac{2\gamma}{\gamma+1}(M_1^2 - 1) \tag{4}$$

The entropy increase through the shock wave is given by

$$\frac{S_2 - S_1}{R} = \ell n \frac{P_{o1}}{P_{o2}} \tag{5}$$

where the ratio of total pressures downstream and upstream of the shock wave is given by

$$\frac{P_{o2}}{P_{o1}} = \left[\frac{\gamma+1}{2\gamma M_1^2-(\gamma-1)}\right]^{\frac{1}{\gamma-1}} \left[\frac{(\gamma+1)M_1^2}{(\gamma-1)M_1^2+2}\right]^{\frac{\gamma}{\gamma-1}} \tag{6}$$

3.3 Profile Drag Derviation

The airfoil section profile drag measurements were computed from the wake survey rake measurements by the method of Refs. [13-15] utilizing the following equations

$$c_d = \int_{\text{wake}}^{c_d'} d\,\frac{h}{c} \tag{7}$$

$$c_d' = 2\left(\frac{H}{H_\infty}\right)^{\frac{\gamma-1}{\gamma}} \left(\frac{P}{P_\infty}\right)^{\frac{1}{\gamma}} \left(\frac{1-\left(\frac{P}{H}\right)^{\frac{\gamma-1}{\gamma}}}{1-\left(\frac{P_\infty}{H_\infty}\right)^{\frac{\gamma-1}{\gamma}}}\right)^{1/2}$$

$$\cdot \left[1-\left(\frac{1-\left(\frac{P_\infty}{H}\right)^{\frac{\gamma-1}{\gamma}}}{1-\left(\frac{P_\infty}{H_\infty}\right)^{\frac{\gamma-1}{\gamma}}}\right)^{1/2}\right] \tag{8}$$

where

H_∞ = free stream total pressure

P_∞ = free stream static pressure

H = local total pressure in the wake

P = local static pressure in the wake

c_d' = point drag coefficient

c_d = section drag coefficient.

To obtain the section drag coefficients, point drag coefficients were computed

for each set of static and total pressure measurements in the wake by using Eq.(8). These point drag coefficients were then summed up according to Eq.(7) by numerical integration across the wake, based on the trapezoidal method.

4. EXPERIMENTAL RESULTS AND DISCUSSIONS

The supercritical airfoil was mounted in the middle of the initial 20 in. of the test section bottom surface, Fig. 1b, with 17 pressure taps distributed along the model surface centerline, Fig. 2a. In Refs. 7 and 8 the flow Mach number in the test section ranged from 0.72 to 0.82, and the drag divergence, or critical, Mach number was about 0.75. By modifying the test section to increase the free stream Mach number in the test section, the effects of porous surface with cavity on the drag reduction were investigated over a free stream range of 0.75 to 0.90 [9,10].

4.1 Schlieren Photographs

The presence of shock wave formations on the surface of the 14%-thick supercritical airfoil were recorded using Schlieren photography. Representative Schlieren photographs taken with a free stream Mach number of 0.806 are presented in Figs. 5a-c for airfoil surface conditions of zero, 1.4% linear and 2.8% uniform porosity. In these photographs the leading and trailing edges of the porous surface are indicated by the vertical dark bars. The normal shock wave existing with the solid airfoil surface, Fig. 5a, is changed to a lambda shock wave, Fig. 5c, by the uniform porosity. Weak disturbances from the holes, even sealed with wax for zero percent porosity, are visible in the photographs because of slight surface irregularity. Also, the slopes of the weak waves indicate that the flow Mach number over the airfoil is approximately 1.2.

a) Zero Porosity

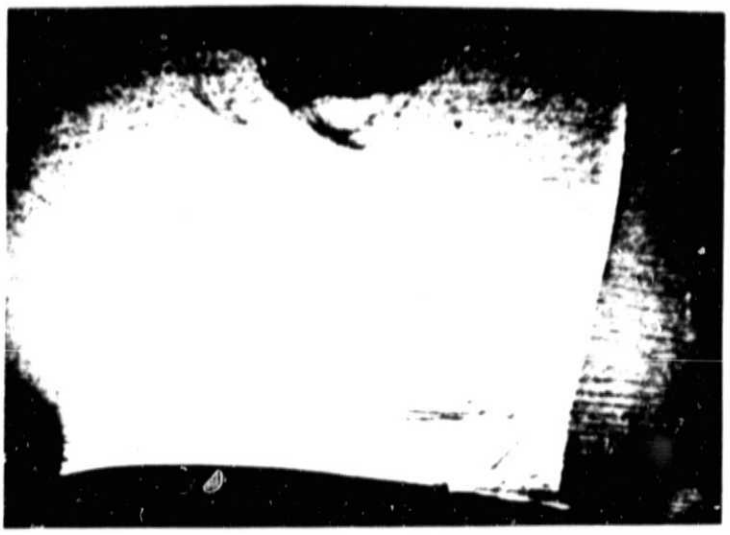

b) 1.4% Linear Porosity

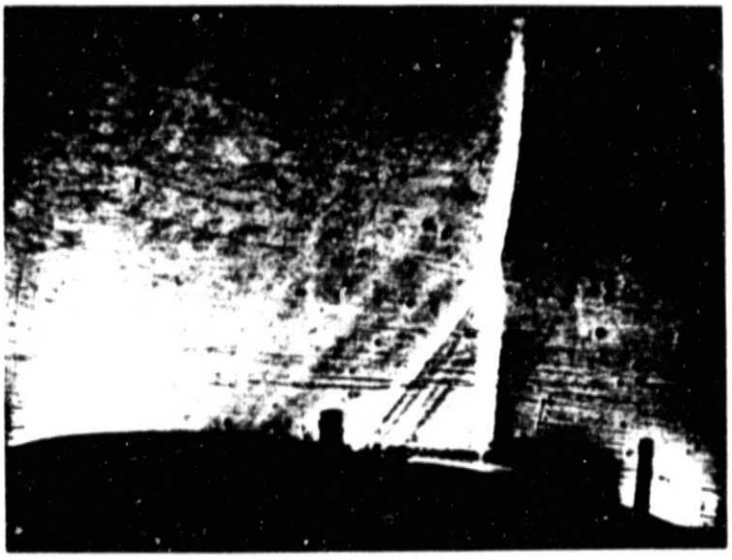

c) 2.8% Uniform Porosity

Fig. 5 Schlieren Photographs of Flow Over Supercritical Airfoil
$M_\infty = 0.806$

For the linear porosity, Fig. 5b, the shape of the shock wave is slightly different than for the solid surface with the location of the inflection point in the shock wave closer to the airfoil surface then for the uniform porosity, Fig. 5c. As discussed earlier, the porous surface with cavity permits a part of the boundary layer to move from the downstream to the upstream of the shock wave location, sending compression waves which produce an oblique shock wave with a terminating normal shock wave. Thus, the flow Mach number in front of the normal shock wave is close to sonic, which is much lower than the case for the solid surface, Fig. 5a.

The Schliern photographs presented are for 0% and 2.8% porosities at a free stream Mach number of 0.85 and are presented in Figs. 6a and b, respectively. In these photographs the flow proceeds from left to right. As described earlier, 0% porosity is the case when all of the holes are plugged. In the discussion of the following photographs note that the .56 to .83 x/c extent of porosity used is clearly makred by two vertical markers in each photograph. The normal shock waves in this case have moved further back to x/c = .71 and the oblique shock wave still originates from the front of the porous region at x/c = .56. The increase in height of the normal shock wave reflects an increase in the height of the supersonic region above the airfoil.

In tests with the free stream Mach number of .87 the normal shock wave for the 2.8% porosity case was located well to the rear of the porous region and that an oblique shock wave still formed emenating from the front of the porous region. This indicates that circulatory flow through the cavity is achieved even when the normal shock wave is located at the end portion of the porous surface.

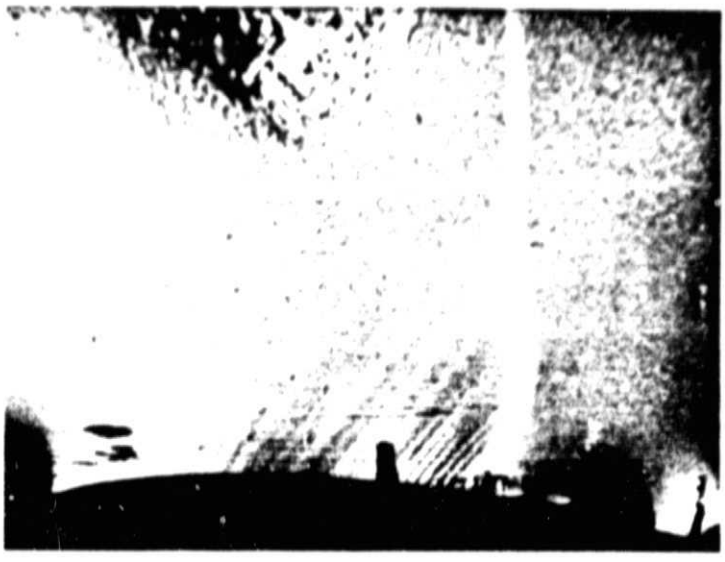

a) Zero Porosity

b) 2.8% Uniform POrosity

Fig. 6 Schlieren Photographis of Flow Over Supercritical Airfoil, $M_\infty = 0.85$, with Top Wall Insert

The x/c locations of the shock waves on the airfoil are plotted versus the free stream Mach number in Fig. 7. This plot clearly shows that the oblique shock wave will always originate from the front of the porous region whenever the normal shock wave is located over the porous surface.

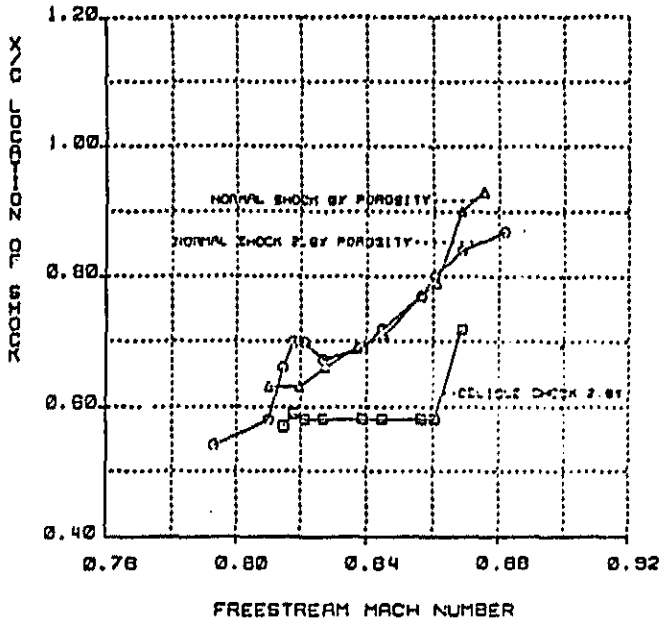

Fig. 7 x/c Position of Shock Waves Versus Freestream Mach Number

4.2 Model Mach Number Distribution

The Mach number distributions over the airfoil surface for 0%, 1.42% linear, and 2.8% uniform porosities and a free stream Mach number of 0.804 were determined from the static pressure measurements and are presented in Fig. 8 for uniform test section [3,4,8]. Surface Mach number distribution remained unaffected by the porosity up to the leading edge of the porous surface because the supersonic flow region starts from approximately 10% of the chord. For the solid surface the maximum Mach number is about 1.24 and the large decrease in Mach number caused by the normal shock wave, Fig. 5a, occurs at about 70% of the chord. The linear porosity of 1.40% decreased the maximum Mach number to about 1.1 and the decrease in the Mach number

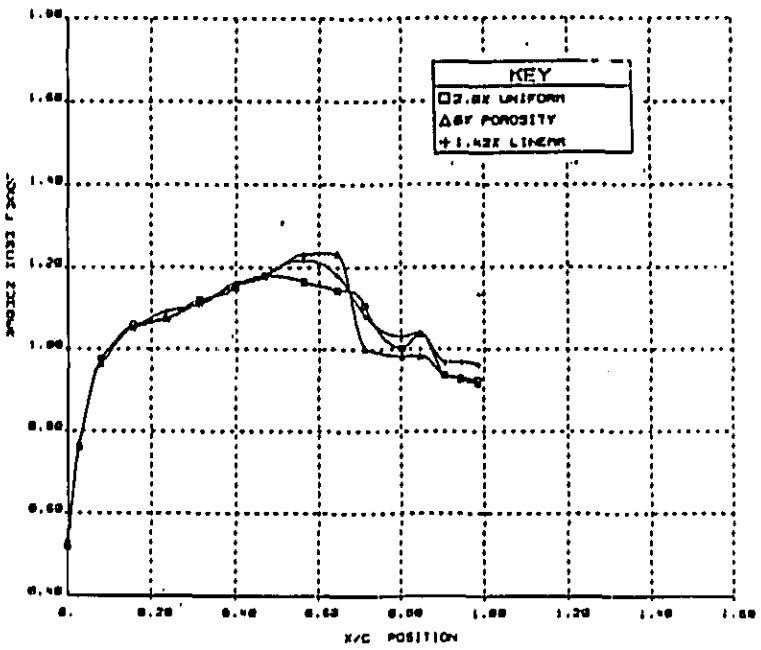

Fig. 8a Mach Number Distribution Over Airfoil with 0%, 1.42% and 2.8% Porosities, M_∞ = 0.804

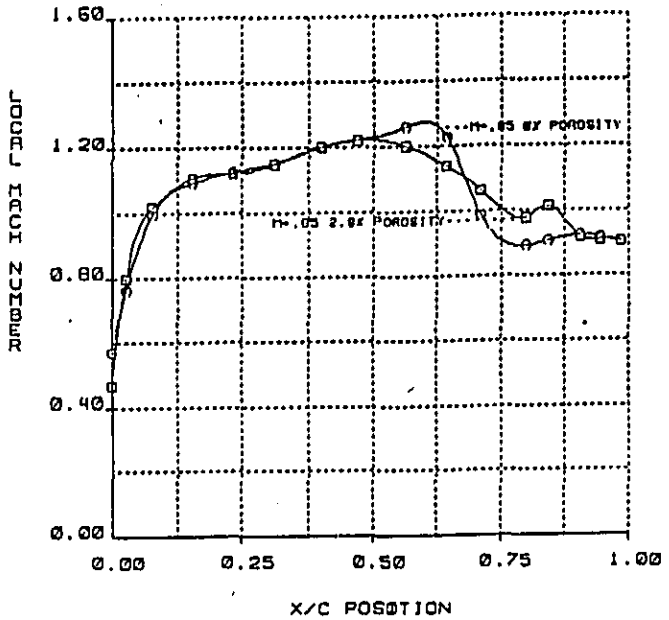

Fig. 8b Mach Number Distribution Over Airfoil with 0% and 2.8% Porosities, M_∞ = 0.85.

due to the normal shock wave, Fig. 5b, was more gradual than for the solid surface.

With the uniform porosity of 2.8% the peak Mach number was decreased to approximatley 1.18 at about 50% chord location and the Mach number decreased to about 1.13 at 70% chord location. This Mach number distribution is due to the oblique shock wave, Fig. 5c, produced by the boundary layer recirculating from downstream of the normal shock with high pressure through the cavity, Fig. 2a, to upstream where the pressure is lower in the supersonic flow region. Downstream from the shock wave, the Mach number is higher with the porosity than without, which corresponds to a decrease in the local pressure and minimizing the flow separation.

Figure 8b shows the Mach number profiles for 0% and 2.8% porosities at a free stream Mach number of 0.85. The nearly vertical drop in Mach number for the 0% porosity cases are again contrasted with the more gradual decreases for the 2.8% porosity cases. Note in Figs. 6a and 6b that the shock wave location is well over the porous region and that the 2.8% porosity case generates a small oblique shock wave for the test section with insert, Fig. 4 [9,10].

4.3 Wake Total Pressure Ratio Distribution

To investigate the effect of the airfoil porous surface on the drag reduction, drag coefficient distributions were calculated from the impact pressure measurements in the wake downstream from the model trailing edge, as shown in Fig. 3 and Eq. (8). Experiments were conducted for a series of free stream Mach numbers. Representative impact pressure surveys for 0% and 2.8% uniform porosity and free a stream Mach number of 0.804 are presented in Fig. 9a. The boundary layer region with low impact pressures for the solid surface extend over appreciable vertical distance, but with the 2.8% uniform porosity the region of low impact pressures is decreased.

This is caused by the boundary layer downstream of the normal shock wave being sucked into the cavity with lower pressure and injected into the flow upstream of the normal shock wave where the pressure in the flow outside

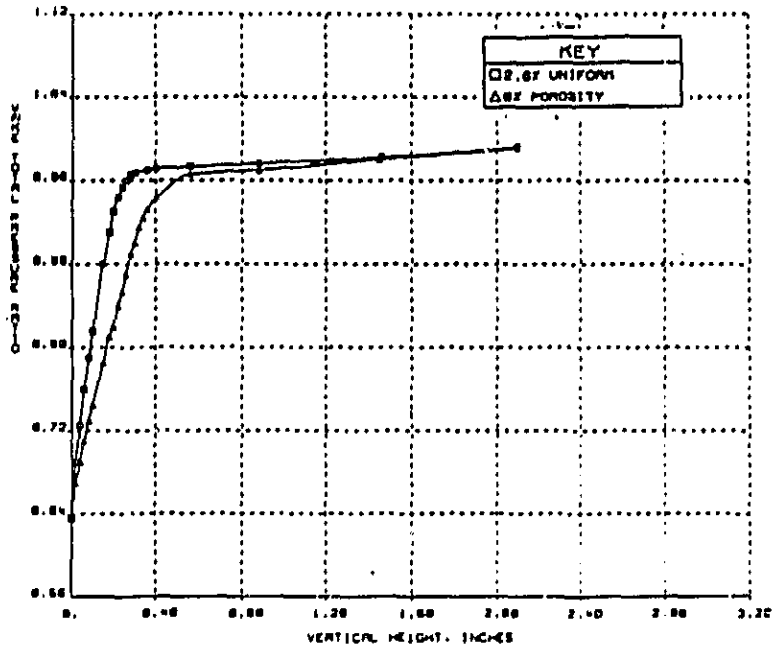

Fig. 9a Wake Total Pressure Ratio Distributions for 0% and 2.8% Uniform Porosities, M_∞ = 0.804.

the cavity is lower.

Figure 9b for a freesteam Mach number of .85 shows that with the normal shock wave located towards the rear of the porous region (cf. Fig. 6b) the 2.8% porosity case yields clearly higher total pressure ratios. It was found that as long as the normal shock wave was located between the center and rear of the porous region a reduction in the point drag coefficients was observed. The amount of porous area located behind the normal shock wave was not as critical to the system's operation because of the higher pressure gradients associcated with these higher Mach numbers.

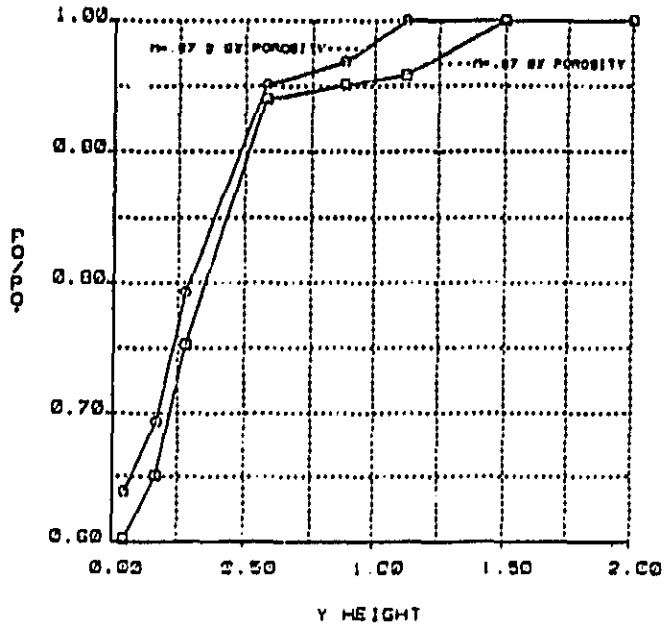

Fig. 9b Wake Total Pressure Ratio Distribution for 0% and 2.8% Prosoities, M_∞ = 0.87

4.4 Drag Variation with Porosity and Mach Number

The upper airfoil section profile drags were calculated from the wake impact presure surveys and using Eqs.(7) and (8) and the results are presented in Fig. 10a for 0%, 1.42% linear, and 2.8% uniform porosities in uniform test section (Fig. 1b) [7,8]. The drag coefficients increased rapidly at high free stream Mach number for all porosities. However, above Mach number of 0.78 the 2.8% uniform porosity showed a dramatic reduction of drag over the 0% porosity by 46% at a Mach number of 0.81. This is due to the compression waves formed by air recirculating through the cavity from behind the main shock wave, lowering the Mach number just in front of the normal shock wave. The thinner boundary layer behind the shock wave helped in keeping the flow to remain attached longer. From the total pressure rake measurements, Fig. 9a, it was observed that the wake of the 2.8% uniform porosity is half the size of the solid surface.

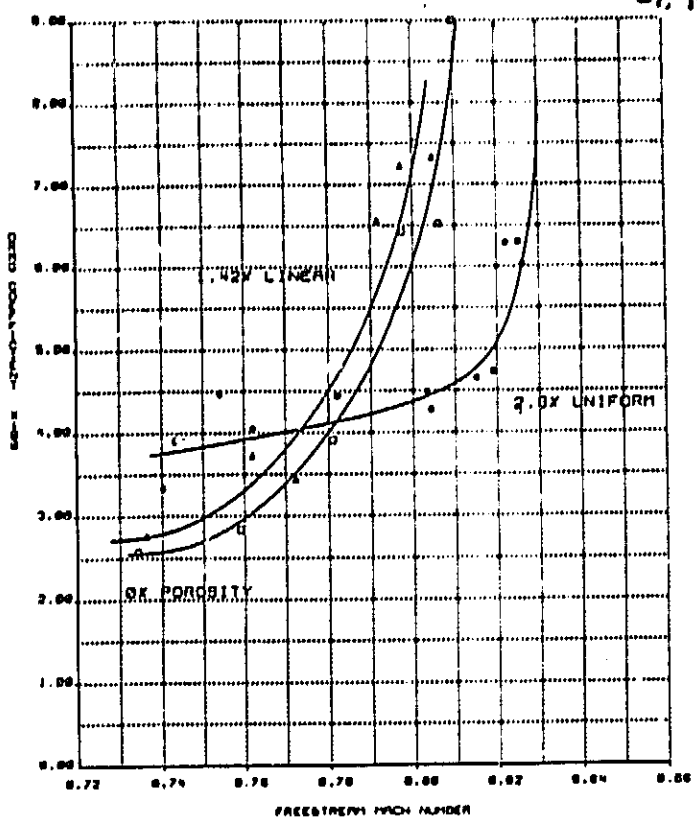

Fig. 10a Drag Coefficient Versus Freestream Mach Number, Comparison of Porosities

Below flow Mach number of 0.78 the 2.8% uniform porosity displayed a higher drag coefficient than for the solid surface. This is possibly due to the surface roughness and the interaction caused by the flow circulating through the cavity, and this can be eliminated by the closing the holes by a sliding valve system. The 1.42% linear porosity failed to reduce the drag; in fact, the drag coefficients were consistently higher than the 0% porosity case. This is again attributed to the roughness on the surface and unexpected flow interaction.

Figure 10b is a plot of the drag coefficient versus free stream Mach number for both 0% and 2.8% porosities with top wall insert, Fig. 4, to increase the free stream Mach number [9,10]. The 2.8% porosity produces slightly higher drag from Mach .75 to .84. In this range there is either

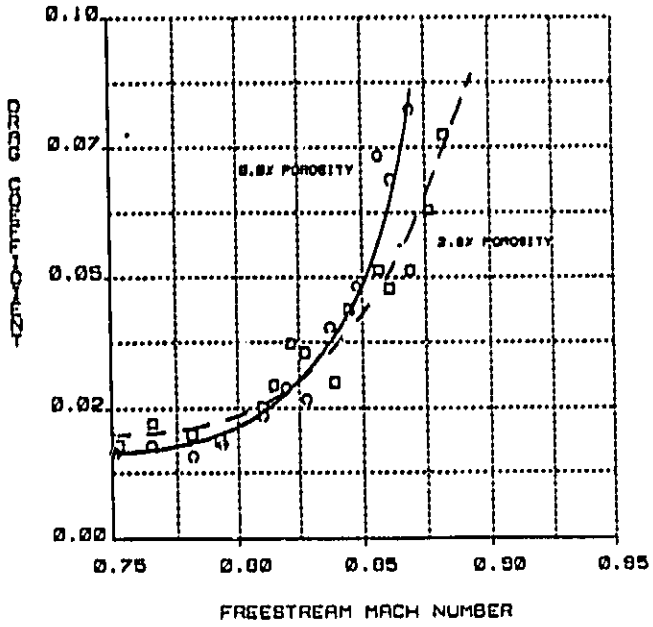

Fig. 10b Drag Coefficient Versus Freestream Mach Number for 0% and .28% Porosities with Top Wall Insert

no shock wave to drive the flow or the shock wave that is present is located ahead of the center region of the porous plate. The slight increases in drag are due to viscous losses from the unsealed holes. From Mach .84 to .88 the 2.8% porosity case yields less drag. The first significant decrease occurs at a free stream Mach number of .84 where the 2.8% case produces 27% less drag then the 0% porosity case.

Higher free stream Mach numbers in the range of .85 to .87 yields 30% to 40% reductions in drag. The maximum drag reduction obtained in this study was 40% at a Mach number of 0.865. Examination of the plot of the total pressure ratio versus y-height for this case in Fig. 9b shows that most of the drag reduction occurs below y = .5 in. This suggests that the boundary layer effects may be more important for drag reduction than the

total pressure losses through the shock waves. The Schlieren photograph for this case (cf. Fig. 6b) shows that the shock wave is located to the rear of the porous surface. Even though this positioning of the normal shock wave allows for a smaller porous surface through which to remove the decelerated flow, the pressure gradient through this shock is still strong enough to establish flow through the cavity.

As discussed earlier these reductions in the drag coefficients can be traced to several elements. First, the flow through the porous region behind the normal shock wave removes the decelerated fluid particles from the boundary layer before they are given a chance to separate. Now the flow emerging out of the porous surface ahead of this shock wave imparts additional energy to the particles of the fluid in the boundary layer near the wall. The fluid particles become accelerated and the danger of separation is reduced [16]. In addition the oblique shock wave triggered by this emerging flow decelerates the flow to a lower supersonic Mach number such that the pressure gradient through the normal shock wave is reduced. This reduced pressure gradient is less likely to separate the boundary layer as discussed in Ref. [9,10].

Active and passive shock wave/boundary interaction control on supercritical airfoils were conducted in Ref. 17 with a double slot and perforated strip configurations with a cavity underneath in the Gottingen IMXIM Transonic Wind Tunnel. Experiments were conducted with and without suction and drag reduction of approximately 40% was observed at transonic Mach number without suction as observed in the present investigation.

5. CONCLUSIONS

5.1 Test Results in 3 in. x 15.4 in. RPI Transonic Wind Tunnel With Constant Cross Section

- An investigation was conducted to study the effects of 0%, 1.42% linear and 2.8% uniform porosities on the 14%-thick supercritical airfoil drag reduction by the passive shock wave/boundary layer control concept. The investigations were conducted over a Mach number range of 0.72 to 0.82.

- The supercritical airfoil was placed on the bottom wall of the test section and a porous surface with a cavity beneath it was positioned from 56% to 81% chord positions. Porsity consisted of 0.025 in. diameter holes spaced uniformly over the 25% chord, making the porosity 2.8% of the total surface area.

- Normal shock wave for the solid surface was changed to an oblique shock wave by the uniform porosity which decreased the entropy increase in the wake and decreased the boundary layer thickness downstream of the normal shock wave. Both of these effects tend to decrease the profile drag.

- Uniformly distributed porosity of 2.8% decreased the upper surface drag approximately 46% at a Mach number of 0.81 compared to the solid airfoil surface. A linearly increasing chordwise distribution of porosity of 1.42% did not decrease the airfoil drag at all Mach numbers.

- At Mach numbers below 0.78 without the shock wave the porous surface increased the drag because of the increased surface roughness effect. This problem can be solved by closing the holes with a sliding valve system.

5.2 Test Results in 3 in. x 15.4 in. RPI Transonic Wind Tunnel With Top Wall Insert

- Passive shock wave/boundary layer control for 0% and 2.8% porosities on a 14% thick supercritical airfoil was investigated in a modified Transonic Wind Tunnel. This modification was necessary to reach free stream Mach numbers above .83. After this change a thorough survey was conducted in the Mach number range of .75 to .90. This included comparisons of Schlieren photographs, model Mach number distributions, and profile drag measurements for both solid surface and 2.8% porosity cases.

- The installation of the top wall insert in the RPI Transonic Wind Tunnel minimized the problems due to boundary layer growth and blockage effects in the test section. In particular, free stream Mach numbers as high as .90 were obtained surpassing the previous limit of .83.

- Schlieren photographs reveal that the 2.8% porosity case will generate an oblique shock wave originating from the front of the porous region as long as the normal shock wave is located over the porous reigon.

- The vertical extent of the normal shock waves increased with increasing free stream Mach number reflecting the growth of the embedded supersonic reigon over the airfoil.

- Model Mach number distributions for both the 0% and 2.8% porosity cases demonstrate that the 2.8% porosity produces less severe drops in the Mach number. This is attributed to the pressure and velocity gradient dampening effect of the porous plate and cavity and the presence of an oblique shock wave.

- For free stream Mach numbers below .83 the 2.8% porosity case produced slightly higher drag coefficients. This increase is attributed to viscous

losses from the porosity. For free stream Mach numbers greater than .83 the 2.8% porosity case led to reductions in the drag coefficient of as much as 40%.

- The normal shock waves for those 2.8% cases that yielded lower drag coefficients were positioned in between the center and rear of the porous region. Those 2.8% cases with the normal shock wave located ahead of the center produced higher drag coefficients. This suggests that the amount of porosity located behind the normal shock wave is not critical to this system's operation as that amount located ahead of this point.

6. RECOMMENDATION FOR NEXT PHASE OF RESEARCH ON PASSIVE SHOCK WAVE/BOUNDARY LAYER CONTROL FOR SUPERCRITICAL AIRFOIL TRANSONIC DRAG REDUCTION

6.1 Porous Surface

- Investigate porous surfaces with holes smaller then 0.025 in. diameter with surface opening of 5 to 10%.

- Determine the length of porous surface for a given airfoil chord required to achieve drag reduction for Mach numbers greater than the critical Mach number.

- Determine the location of the porous surface relative to the normal shock wave for the solid airfoil to produce maximum drag reduction for transonic Mach numbers.

6.2 Geometry of the Cavity Below the Porous Surface

- Investigate the minimum depth of the cavity below the porous surface for maximum drag reduction for transonic Mach numbers.

- Determine the optimum cavity geometry to achieve maximum transonic drag reduction.

6.3 Supercritical Airfoil Placed in the Center of the Transonic Wind Tunnel With Contoured Top and Bottom Walls

- Calculate the supercritical airfoil flow field in free space and use this information to contour the top and bottom walls with boundary layer correction to simulate free flight conditions.

- Construct adjustable top and bottom wind tunnel walls to simulate the streamlines for free flight conditions.

- Investigate the porous surface and cavity geometry for the supercritical airfoil to produce maximum transonic drag reduction as functions of Mach number and lift coefficient.

- Determine the airfoil surface pressure and Mach number distributions, Schlieren photographs of shock wave shapes and boundary layer, and wake impact pressure distribution for the supercritical airfoil with porosity and cavity.

7. LITERATURE CITED

1. Nixon, D., "Design of Transonic Airfoil Sections Using A Similiarity Theory," NASA Ames Research Center, Moffet Field, CA, 17th Aerospace Sciences Meeting, New Orleans, LA, January 15-17, 1979.

2. Harris, C.D., R.J. MeGhee and D.O. Allison, "Low-Speed Aerodynamic Characteristics of a 14% Thick NASA Phase 2 Supercritical Airfoil Designed for Lift Coefficient of 0.7," NASA TM 81912, December 1980.

3. Ross, J.M., "Passive Shock Wave/Boundary Layer Control for Drag Reduction of a Convex Transonic Airfoil," Master's Thesis, Rensselaer Polytechnic Institute, May 1982.

4. Bahi, L., "Passive Shock Wave/Boundary Layer Control for Transonic Supercritical Airfoil Drag Reduction," Ph.D. Thesis, Rensselaer Polytechnic Institute, May 1982.

6. Bidlack, T., "Top Wall Blockage Effects on Passive Shock Wave Boundary Layer Control for Supercritical Airfoil," M.S. Thesis Rensselaer Polytechnic Institute, Aug. 1982.

7. Orozco, R.D., "Porosity Effects on Supercritical Airfoil Drag Reduciton By Shock Wave/Boundary Layer Control," M.S. Thesis, Rensselaer Polytechnic Institute, May 1983.

8. Nagamatsu, H.T., Orozco, R.D., and Ling, D.C., "Porosity Effect on Supercritical Airfoil Drag Reduction by Shock Wave/Boundary Layer Control," AIAA Paper No. 84-1682.

9. Ficarra, R., "Supercritical Airfoil Drag REduction by Passive Shock Wave/Boundary Layer Control in the Mach Number Range 0.75 to 0.90," M.S. Thesis, Rensselaer Polytechnic Institute, Troy, New York, May 1984.

10. Nagamatsu, H.T., Ficarra, R.V., and Dyer, R., "Supercritical Airfoil Drag Reduction by Passive Shock Wave/Boundary Layer Control in the Mach Number Range 0.75 to 0.90," AIAA Paper No. 85-0207, Jan. 1985.

11. Liepmann, H.W., "The Interaction Between the Boundary Layer and SHock Waves
in Transonic Flow," Jour. of Aero., Sci. Vol. 13, pp. 623-638, December 1946.

12. Ames Research Staff, "Equations and Charts for Compressible Flow," NASA Rept. 1135.

13. Lock, C., W. Hilton and S. Goldstein, "Determination of Profile Drag at High
Speeds by a Pitot Transverse Method," Reports and Memoranda No. 1971, British A.R.C., September 1940.

14. Silverstein, A. and S. Katzoff, "A Simplified Method for Determiining Wing Profile Drag in Flight," Journal of Aeronautical Science, 7, 7 (May 1940).

15. Pankhurst, R.C. and D.W. Holder, Wind Tunnel Technique, Sir Issac Pitman and Sons, Ltd., London 1965.

16. Schlichting, H., Boundary Layer Theory, McGraw-Hill, New York, 1955.

17. Thiede, P., Krogmann, P., and Stanewsky, E., "Active and Passive Shock/Boundary Layer Interaction Control on Supercritical Airfoils," AGARD Symposium on Improvement of Aerodyanmic Performance Through Boundary Layer Control and High Lift Systems," May 23, 1984.